



Citation	<p>Min Lia, Duncan den Boer, Patrizia Iavicoli, Jinne Adisoejoso, Hiroshi Uji-i, Mark Van der Auweraer, David B. Amabilino, Johannes A.A.W. Elemans and Steven De Feyter</p> <p>Tip-Induced Chemical Manipulation of Metal Porphyrins at a Liquid-Solid Interface</p> <p>Journal of the American Chemical Society, 2014, 136, 17418 – 17421</p>
Archived version	<p>Author manuscript: the content is identical to the content of the published paper, but without the final typesetting by the publisher</p>
Published version	<p>insert link to the published version of your paper</p> <p>http://dx.doi.org/10.1021/ja510930z</p>
Journal homepage	<p>insert link to the journal homepage of your paper</p> <p>http://pubs.acs.org/journal/jacsat</p>
Author contact	<p>your email steven.defeyter@kuleuven.be</p> <p>your phone number + 32 (0)16 327921</p>
IR	<p>url in Lirias https://lirias.kuleuven.be/handle/123456789/481734</p>

(article begins on next page)



Tip-Induced Chemical Manipulation of Metal Porphyrins at a Liquid-Solid Interface

Min Li^{a,b,‡}, Duncan den Boer^{c,‡}, Patrizia Iavicoli^{dt}, JinneAdisojojoso,^a Hiroshi Uji-i^a, Mark Van der Auweraer^a, David B. Amabilino^{d§*}, Johannes A.A.W. Elemans^{c*} and Steven De Feyter^{a*}

^aKU Leuven - University of Leuven, Division of Molecular Imaging and Photonics, Celestijnenlaan 200-F, 3001 Leuven, Belgium

^bCAS Key Laboratory for Biomedical Effects of Nanomaterials and Nanosafety, Institute of High Energy Physics, Chinese Academy of Sciences, Beijing, 100049, China

^cRadboud University Nijmegen, Institute for Molecules and Materials (IMM), Heyendaalseweg 135, 6525 AJ Nijmegen, The Netherlands

^dInstitut de Ciència de Materials de Barcelona (ICMAB-CSIC), Campus Universitari, 08193 Bellaterra, Catalonia, Spain

[§]Present address: School of Chemistry, The University of Nottingham, Nottingham NG7 2RD, UK

[†]Present address: European Commission Joint Research Centre, Via Enrico Fermi 2749, 21027 Ispra (VA), Italy

Supporting Information Placeholder

ABSTRACT: Changing abruptly the potential between a scanning tunneling microscope (STM) tip and a graphite substrate induces "high-conductance" spots at the molecular level in a monolayer formed by a manganese chloride porphyrin molecule (Mn(III)-PP). These events are attributed to the pulse-induced formation of μ -oxo-porphyrin dimers. The pulse voltage must pass a certain threshold for dimer formation and pulse polarity determines the yield.

plied to the STM tip.^{18,19} In addition, metal atomic manipulations on surfaces induced by a voltage pulse have been studied by STM, where the diffusion of the metal atoms was attributed to a lower activation energy caused by the voltage pulse.^{20,21} Furthermore, voltage pulses can also provoke reversible single-molecule switching^{22,23} and conformational changes of the adsorbed molecules on surfaces.^{24,25}

Scanning tunneling microscopy (STM) has proven to be a powerful technique to obtain spatial information at the atomic level and can be used to investigate dynamics and chemical phenomena on surfaces,¹⁻⁷ which is essential to explore the details of interfacial reaction processes involving single molecules.^{8,9} The STM tips can also be used to initiate local reactions.¹¹⁻¹⁶ For instance, one-dimensional chain polymerization has been initiated by a voltage pulse applied to an STM tip during scanning.^{11,16} It was also demonstrated that the polymerization of C₆₀ into ring-like features can be induced.¹⁷ The dissociation of molecules adsorbed on metal surfaces can be initiated as well, which originates from a voltage pulse ap-

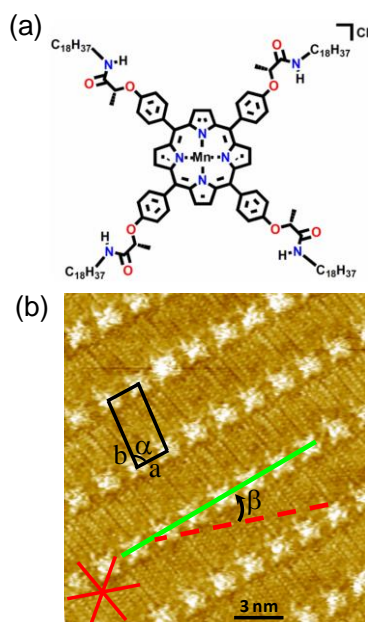


Figure 1. Molecular structure of Mn(III)-PP and its self-assembly pattern on graphite. (a) Chemical structure of Mn(III)-PP. (b) STM constant-current image (tunneling current $I = 0.05$ nA, sample bias: $V_s = -0.8$ V) of a Mn(III)-PP monolayer self-assembled at a 1-octanoic acid/HOPG interface. Rows of porphyrin molecules do not run parallel to a main graphite axis but deviate by $\beta = -21 \pm 2^\circ$ from this reference axis as shown in Figure 1b. Both the unit cell parameters ($a = 1.9 \pm 0.1$ nm, $b = 4.0 \pm 0.1$ nm, $\alpha = 83 \pm 2^\circ$), and chiral expression are similar to the free base analogue of Mn(III)-PP.²⁶

Most of these tip-induced reactions have been carried out under ultra-high vacuum (UHV) conditions. Liquid-solid interfaces are more complex as reactions are not by definition confined to molecules adsorbed on the surface. While this could be considered as a drawback, it also opens new possibilities for reactivity. Here, we report a localized STM-tip induced reaction of a manganese chloride porphyrin (Mn(III)-PP, Figure 1a) monolayer upon applying a voltage pulse at the liquid/solid interface between 1-octanoic acid and graphite, and reveal the importance of pulse height, polarity, and the presence of oxygen in the atmosphere on the outcome of the reaction.

Mn(III)-porphyrins are well-known as catalysts in a wide range of oxidation reactions.²⁷ We have recently succeeded in detecting with STM different oxidation states of individual manganese porphyrins during their reaction with oxygen at a solid/liquid interface.²⁸ When a solution of Mn(III)-PP in 1-octanoic acid (10^{-5} M) was drop-cast at room temperature on the basal plane of highly oriented pyrolytic graphite (HOPG), a well-organized physisorbed monolayer was formed, as revealed by STM imaging in the liquid (Figure 1b). Similar to its free base porphyrin analogue, Mn(III)-PP arranges in rows in which the alkyl chains interdigitate into a densely packed structure.²⁶

Upon applying several voltage pulses (pulse height: $P_s = -4.5$ V, pulse width: $P_w = 100$ μ s) to the STM tip at different locations of the scanning area, the emergence of many spots much brighter than the as-deposited compound are seen clearly in

the monolayer (Figure 2a). The bright spots were observed exactly at the position of the Mn(III)-PP core in the monolayers (Figure 2a), and measured approximately 0.8 nm in height, as shown in Figure 2b. One should note that the apparent height of the bright spot varies significantly between experiments (See Figure S1). In our previous work, the bright spot is measured to be 500 pm in height at lower set-point, that is, 10 pA.²⁸ In Figure 2c, the result of a single pulse experiment is shown. The yellow line indicates the distribution of the bright spots in a local domain after one single negative substrate pulse (pulse voltage to the sample: $P_s = -4.5$ V, pulse width: $P_w = 100$ μ s, retracting the STM tip by 15 Å before pulsing). The pulse position is indicated by the green cross. The asymmetry of the tip geometry plays a role in the reaction. Specifically, it could give rise to an observed uneven distribution of product species because of the inhomogeneous electric field as presented in Figure S2c. Worthy of note is that though the bright spot formation was the main focus in this work, species with a lower contrast²⁸ could still be observed as shown in Figure S3.

Figure 3a shows a histogram of single-pulse experiments ($P_s = -4.5$ V; $P_w = 100$ μ s; substrate bias (V_s) = -0.8 V) reflecting the number of bright spots as a function of the distance from the pulse location. On average, ~ 5 – ~ 7 high-conductance spots are generated per pulse. This histogram is based on the data obtained in the first full scan (complete STM image) after the pulse. Note that the bright spots are demonstrated to be stable within several consecutive scans (Figure S4). The spots were observed in a radial distribution surrounding the location of the pulse. Based on Figure 3a, about 86% of the high-conductance spots appear within a radius of 30 nm from the pulse location (the total number of the collected bright spots is 259, of which 222 appeared within a radius of 30 nm). Note that the actual percentage could be higher, due to the following: The low yield of spots close to the pulse location (see for example the bars between 0–10 nm in Figure 3a) is not attributed to a reduced efficiency, but to an induced desorption of part of the monolayer in the direct vicinity of the pulse location (Figure S2).^{4, 29} Typically, the radius of the desorbed domain after one pulse is 13 ± 5 nm (Figure S2a), and it takes seconds to minutes to refill. Note that once (re)adsorbed, the degree of dynamics in the monolayer is very low (Figure S4), which is in line with observations for other porphyrin monolayers^{30, 31a} and is consistent with observations of kinetic control in layer assembly.³¹ In a next series of experiments, we investigated the dependence of the appearance of the bright spots upon applying the pulse voltage, in terms of pulse height and polarity. From the graph in Figure 3b it is apparent that 1) at both pulse voltage polarities, bright spots are induced; 2) a larger magnitude of the pulse voltage, up till ± 5.5 V, leads to more spots; 3) at both polarities a threshold voltage (~ 2 – 3 V) is observed before the spots appear; 4) there is a yield dependency on the pulse voltage polarity: at negative substrate pulse voltages the yield is higher by about a factor of three.

The yield of the bright spots upon pulsing drops very fast with increasing the tip-sample distance. When the retract distance of the STM tip before pulsing is 1.5 nm, a significant number of bright spots are induced. From 50 nm on, the yield drops dramatically to about one bright spot per pulse or no bright spots at all (Figure S5).

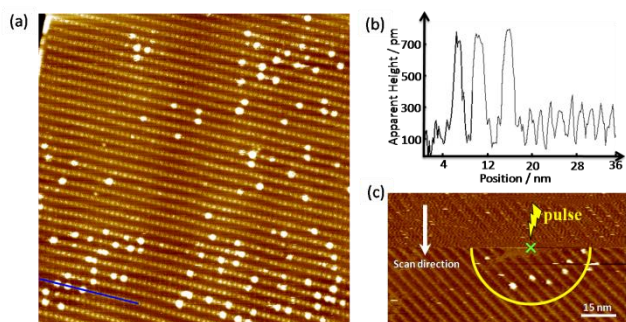


Figure 2. (a) STM image (108 nm \times 108 nm) of a monolayer of Mn(III)-PP at the 1-octanoic acid/HOPG interface obtained after applying several pulses ($P_s = -4.5$ V). Many high conductance spots appear. (b) Line profile along the blue line in (a). (c) STM image with bright spots, resulting from a single pulse. The pulse position is indicated by the green cross. The yellow line indicates the area affected, i.e. the area where bright spots are observed, after one single pulse. Scanning conditions are $I = 0.05$ nA, $V_s = -0.8$ V; $P_s = -4.5$ V, Pulse width: 100 μ s; retract distance of the STM tip before pulsing: 15 \AA .

Knowing that Mn-porphyrins show reactivity towards molecular oxygen, some pulse experiments were not carried out under ambient laboratory conditions but under an Ar atmosphere (see Figure S7). A drastic decrease in the number of the bright spots appearing at a pulse voltage of -4.5 V was observed, with typically 0 to 2 remaining induced bright spots per pulse (see Figure S7b), which we attribute to a small remaining oxygen content in the solution.

The topographical signature in combination with the apparent height suggests a dimeric porphyrin structure.²⁸ Together with the observed oxygen dependence, we propose that the bright states correspond to μ -oxo dimers, which are well-known products of the reaction of Mn-porphyrin with oxygen.³² We have recently detected these species during STM studies of Mn(III)-PP²⁸ and by applying very low tunneling currents the characteristic four-leaf clover structure of the top porphyrin could be sub-molecularly resolved (Figure S8). Surface-bound μ -oxo Mn-porphyrin dimers have been proposed to form via a multistep reaction (Scheme 1), in which first a surface-bound Mn(III)-porphyrin is reduced to a Mn(II)-porphyrin,^{28,33} which subsequently reacts with oxygen to generate a Mn-dioxo species. After dissociation of the oxygen-oxygen bond, a reactive Mn(IV)-oxo intermediate is formed,³⁴ which can subsequently react with an additional Mn(III)-porphyrin. This reaction could happen from solution to form, upon the addition of an extra electron, the μ -oxo dimer if it is surface bound, or vice-versa if it is a dissolved Mn(IV)-oxo species that reacts with an Mn(III)-porphyrin on the surface.

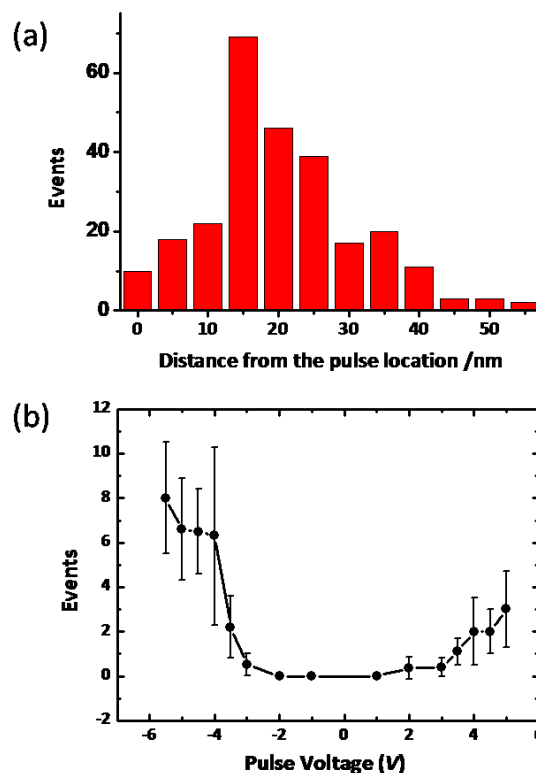
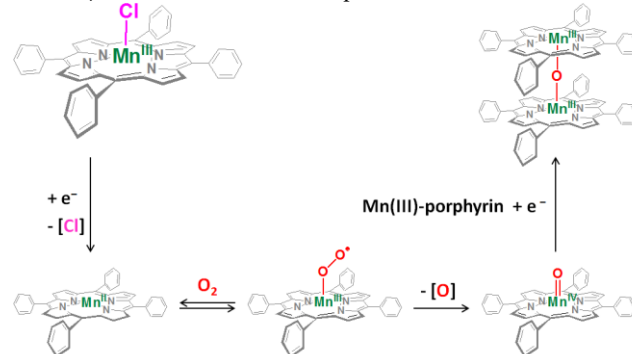


Figure 3. (a) Histogram of 48 single-pulse experiments ($P_s = -4.5$ V, 100 μ s, 15 \AA ; $V_s = -0.8$ V; $I = 0.05$ nA) reflecting the number of bright spots as a function of the distance from the pulse location. (b) Yield of the bright spots as a function of the voltage of a single pulse to the sample, for $V_s = -0.8$ V. For histograms of the number of bright spots per pulse for the different pulse voltages, see Figure S6 and Table S1.

The application of a voltage pulse can explain both the delivery of the two electrons and the second porphyrin needed for the formation of the Mn-porphyrin μ -oxo dimer products, as well as the specific locations of these formed dimers. Several factors can play an important role. (i) During the pulse, “hot electrons” are present in the tunneling current that might have sufficient energy to enable a reduction of Mn(III) porphyrins, at the surface, as well as in the solution.³⁵ However, as μ -oxo dimeric products have been



Scheme 1. Formation of a Mn-porphyrin μ -oxo dimer via a multistep reaction.

observed as far as 50 nm from the location of the pulse (see Figure 3a), it is unlikely that the tunneling electrons are the sole cause of the reaction. Since the self-assembled monolayer is formed on graphite and not on a metal surface, the injection of hot carriers into the substrate^{8,19} is unlikely. (2) An electric field has been found to change effectively intermolecular potentials¹⁹ and this could change the energy landscape of a chemical reaction.²⁵ (3) The applied voltage during the pulse leads also to a high induced charge on the tip apex and a nearby surface. The electronic coupling between the molecules and the surface can be expected to be higher than with the tip. Therefore, electrons induced by a negative pulse on the surface will be more likely to reduce a Mn(III)-porphyrin than those electrons induced on the tip by a positive pulse, which could explain the higher yield at negative pulse voltages (Figure 3b). Furthermore, the difference between work function of the graphite surface (4.6 eV) and the platinum-iridium (Pt/Ir) alloy tip (5.7 eV) also makes it more likely for the Mn(III)-PP molecules to obtain an electron from the graphite surface. (4) The pulse also leads to a very high inhomogeneous electric field near the tip apex, which may attract the polarizable Mn porphyrins in solution, leading to a high local concentration.³⁶ This would explain the relatively high abundance of Mn-porphyrin μ -oxo dimers (and not single Mn-porphyrin oxo complexes) close to the location of the pulse. (5) At the pulse location it would be no surprise if a lot of Mn(III) to Mn(II) reductions occur, and at the same time molecules are "blown away" from the surface into solution. Mn(II) porphyrins are very reactive towards O₂. If then O-O splitting occurs (perhaps still because of the pulse), the resulting porphyrin Mn(IV)=O species may well land on another, remote porphyrin to form a μ -oxo dimer. (6) The reactive porphyrin intermediates, generated as a result of the pulse, apparently have faster reaction kinetics with porphyrins in the non-desorbed part of the layer than the re-adsorption kinetics at the desorption spot. In the non-desorbed domain, the exchange of adsorbed porphyrins with those in solution is limited (see Figure S4), and the observed μ -oxo Mn-porphyrin dimer products are therefore expected to be mostly formed on the surface. Close to the pulse location, however, desorption and re-adsorption of porphyrins play a prominent role. In the case that a reactive porphyrin intermediate reacts with a porphyrin in solution, the resulting μ -oxo Mn-porphyrin dimer product can either diffuse away, or re-adsorb at the location of the pulse. Combined with the fact that a substantial amount of unreacted Mn(III)-porphyrins is also still present in solution, and competes for adsorption, the relative abundance of re-adsorbed μ -oxo Mn-porphyrin dimers on the surface is expected to be lower close to the pulse location than at the surrounding non-desorbed area (which is in line with the observations depicted in Figure 3a.).

In summary, we have been able to induce a local chemical reaction on a surface by applying a pulse voltage with the STM tip. The yield dependence of the bright dots on the pulse voltage and pulse polarity were investigated thoroughly. Based on the results of the atmosphere-control experiments, we pro-

pose here that the bright dots are related to oxidation products of Mn(III)-PP, that is μ -oxo dimers, which is consistent with our previous study.²⁸ This work opens the way to manipulate reactions locally at the nanoscale, in particular at liquid-solid interfaces.

ASSOCIATED CONTENT

Supporting Information

Additional experimental section, STM images and data analysis. This material is available free of charge via the Internet at <http://pubs.acs.org>.

AUTHOR INFORMATION

Corresponding Author

*To whom correspondence should be addressed; E-mail: Steven.DeFeyter@chem.kuleuven.be (S.D.F.); J.Elemans@science.ru.nl (J.A.A.W.E.); David.Amabilino@nottingham.ac.uk (D.B.A.).

Author Contributions

‡These authors contributed equally.

ACKNOWLEDGMENTS

J.A.A.W.E. and D.d.B. thank NanoLab Nijmegen and the Council for the Chemical Sciences of The Netherlands Organisation for Scientific Research (CW-NWO) for a Vidi grant (700.58.423). J.A.A.W.E. thanks the European Research Council for an ERC Starting Grant (NANOCAT – 259064) and the Dutch Ministry of Education, Culture and Science (Gravity program 024.001.035). S.D.F. thanks the Fund of Scientific Research Flanders (FWO), KU Leuven for providing a GOA grant, and the Belgian Federal Science Policy Office (IAP 7/05). This research has also received funding from the European Research Council under the European Union's Seventh Framework Programme (FP7/2007-2013)/ERC Grant Agreement no. 340324. M.L. acknowledges the Fund from the National Natural Science Foundation of China (grant no. 21303208), and the National Basic Research Program (973 Program) of China (No. 2011CB933101).

REFERENCES

1. Okawa, Y.; Aono, M. *Nature* **2001**, *409*, 683.
2. Grill, L.; Dyer, M.; Lafferentz, L.; Persson, M.; Peters, M. V.; Hecht, S. *Nat. Nanotechnol.* **2007**, *2*, 687.
3. Gimzewski, J. K.; Joachim, C. *Science* **1999**, *283*, 1683.
4. Gaudioso, J.; Lee, H. J.; Ho, W. *J. Am. Chem. Soc.* **1999**, *121*, 8479.
5. Lopinski, G. P.; Wayner, D. D. M.; Wolkow, R. A. *Nature* **2000**, *406*, 48.
6. Heinz, R.; Stabel, A.; Rabe, J. P.; Wegner, G.; De Schryver, F. C.; Corens, D.; Dehaen, W.; Suling, C. *Angew. Chem. Int. Ed.* **1994**, *33*, 2080.
7. Abdel-Mottaleb, M. M. S.; De Feyter, S.; Gesquiere, A.; Siefert, M.; Klapper, M.; Müllen, K.; De Schryver, F. C. *Nano Lett.* **2001**, *1*, 353.
8. Maksymovych, P.; Sorescu, D. C.; Jordan, K. D.; Yates, J. T. *Science* **2008**, *322*, 1664.
9. Ho, W. *J. Chem. Phys.* **2002**, *117*, 11033.

10. Dujardin, G.; Walkup, R. E.; Avouris, P. *Science* **1992**, 255, 1232.
11. Stipe, B. C.; Rezaei, M. A.; Ho, W.; Gao, S.; Persson, M.; Lundqvist, B. I. *Phys. Rev. Lett.* **1997**, 78, 4410.
12. Ho, W. *Acc. Chem. Res.* **1998**, 31, 567.
13. Lee, H. J.; Ho, W. *Science* **1999**, 286, 1719.
14. Repp, J.; Meyer, G.; Paavilainen, S.; Olsson, F. E.; Persson, M., *Science* **2006**, 312, 1196.
15. Lastapis, M.; Martin, M.; Riedel, D.; Hellner, L.; Comtet, G.; Dujardin, G. *Science* **2005**, 308, 1000.
16. Miura, A.; De Feyter, S.; Abdel-Mottaleb, M. M. S.; Gesquiere, A.; Grim, P. C. M.; Moessner, G.; Sieffert, M.; Klapper, M.; Müllen, K.; De Schryver, F. C. *Langmuir* **2003**, 19, 6474.
17. Nouchi, R.; Masunari, K.; Ohta, T.; Kubozono, Y.; Iwasa, Y. *Phys. Rev. Lett.* **2006**, 97, 196101/1.
18. Chen, L.; Li, H.; Wee, A. T. S. *ACS Nano* **2009**, 3, 3684.
19. Maksymovych, P.; Dougherty, D. B.; Zhu, X. Y.; Yates, J. T. *Phys. Rev. Lett.* **2007**, 99, 016101-1.
20. Tsong, T. T. *Phys. Rev. B* **1991**, 44, 13703.
21. Hasegawa, Y.; Avouris, P. *Science* **1992**, 258, 1763.
22. Huang, Y. L.; Lu, Y. H.; Niu, T. C.; Huang, H.; Kera, S.; Ueno, N.; Wee, A. T. S.; Chen, W. *Small* **2012**, 8, 1423.
23. Zhang, J. L.; Xu, J. L.; Niu, T. C.; Lu, Y. H.; Liu, L.; Chen, W. *J. Phys. Chem. C* **2014**, 118, 1712.
24. Boland, J. J. *Science* **1993**, 262, 1703.
25. Alemani, M.; Peters, M. V.; Hecht, S.; Rieder, K. H.; Moresco, F.; Grill, L. J. *Am. Chem. Soc.* **2006**, 128, 14446.
26. Linares, M.; Iavicoli, P.; Psychogiopoulou, K.; Beljonne, D.; De Feyter, S.; Lazzaroni, R. and Amabilino, D. B. *Langmuir*, **2008**, 24, 9566. Note that a different reference axis is used.
27. Meunier, B. *Chem. Rev.* **1992**, 92, 1411.
28. den Boer, D.; Li, M.; Habets, H.; Iavicoli, P.; Rowan, A. E.; Nolte, R. J. M.; Speller, S.; Amabilino, D. B.; De Feyter, S.; Elemans, J. A. A. W. *Nat. Chem.* **2013**, 5, 621
29. Wang, C.; Bai, C. L.; Li, X. D.; Shang, G. Y.; Lee, I.; Wang, X. W.; Qiu, X. H.; Tian, F. *Appl. Phys. Lett.* **1996**, 69, 348.
30. Coenen, M. J. J.; Cremers, M.; den Boer, D.; van den Bruele, F. J.; Khoury, T.; Santic, M.; Crossley, M. J.; van Enckevort, W. J. P.; Hendriksen, B. L. M.; Elemans, J. A. A. W.; Speller, S. *Chem. Commun.*, **2011**, 47, 9666.
31. (a) Bhattarai, A.; Mazur, U.; Hipps, K. W. *J. Am. Chem. Soc.* **2014**, 136, 2142; (b) Friesen, B. A.; Bhattarai, A.; Mazur, U.; Hipps, K. W. *J. Am. Chem. Soc.* **2012**, 134, 14897.
32. (a) Feiters, M. C.; Rowan, A. E.; Nolte, R. J. M. *Chem. Soc. Rev.* **2000**, 29, 375; (b) Meunier, B. *Chem. Rev.* **1992**, 92, 1411; (c) Lyons, J. E., Ellis, P. E. & Myers, H. K. *J. Catal.*, **1995**, 155, 59.
33. Hulsken, B.; Van Hameren, R.; Gerritsen, J. W.; Khoury, T.; Thordarson, P.; Crossley, M. J.; Rowan, A. E.; Nolte, R. J. M.; Elemans, J. A. A. W.; Speller, S. *Nat. Nanotechnol.* **2007**, 2, 285.
34. Tabushi, I. *Coord. Chem. Rev.*, **1988**, 86, 1.
35. (a) Smejtek, P. and Silver, M. J. *Phys. Chem.* **1972**, 76, 3890; (b) Cizek, M.; Horacek, J.; Allan, M.; Fabrikant, II; Domcke, W. *J. Phys. B: At. Mol. Opt. Phys.* **2003**, 36, 2837; (c) Sze, S. M.; Crowell, C. R.; Carey, G. P.; Labate, E. E. *J. Appl. Phys.* **1966**, 37, 2690.
36. (a) Fuchsel, G.; Klamroth, T.; Dokic, J.; Saalfrank, P. J. *Phys. Chem. B* **2006**, 110, 1633736. (b) Ni, K.-K.; Ospelkaus, S.; Wang, D.; Quémener, G.; Neyenhuis, B.; Miranda, M. H. G. D.; Bohn, J. L.; Ye, J. & Jin, D. S. *Nature*, **2010**, 464, 1324

(Word Style "TF_References_Section"). References are placed at the end of the manuscript. Authors are responsible for the accuracy and completeness of all references. Examples of the recommended formats for the various reference types can be found at <http://pubs.acs.org/page/4authors/index.html>. Detailed information on reference style can be found in The ACS Style Guide, available from Oxford Press.

Insert Table of Contents artwork here

